Measurement of α-Synuclein net charge in the presence of divalent cations

Mattias Akke, Matthias Schneider, Therese Herling, Tuomas Knowles
Cambridge University, Centre for Protein Misfolding Diseases Email: *mattias.akke@gmail.com

***Abstract*—The interactions between amyloids and metal cations may play an important role in the underlying mechanisms behind several neurodegenerative diseases. We therefore tried to probe, and characterise, interactions between α-Synuclein (αS) and divalent cations using microfluidic free-flow electrophoresis and diffusion sizing. More precisely, we investigated αS at pH 5.5, 6, 6.5, and 7, and its interactions with Ca^{2+} and Cu^{2+}. Due to time restrains, we only accurately measured the charge of αS at pH 7. However, there are several interesting takeaways from this study. Under the solution conditions used here, we did not observe any interactions between Ca^{2+} and αS, but we did observe significant interactions between Cu^{2+} and αS.**

I. Introduction

Neurodegenerative diseases are one of the fastest increasing causes of death in the world [1]. They are commonly linked to increased levels of intrinsically disordered proteins in the brain, such as amyloid-β in Alzheimers patients and α-Synuclein in Parkinson's patients. The molecular interactions that underlie the disease is, although extensively studied, still largely unknown. There is a growing interest in the role of metal ions in neurodegenerative diseases. Several d-block metal ions have been linked to critical processes in amyloid-β aggregation and pathogenesis [2], and they have been shown to play a role in the induction of radical oxidative species (ROS) caused by αS oligomers [1], [3]. Determining the net charge of monomers in the presence of different metal cations and at different pH could provide valuable insight into amyloid-ion interactions.

Ca^{2+} and Cu^{2+} are especially interesting, and both have been extensively studied both *in-vivo* and *in-virto*. Some patients with Parkinssons have been found to have increased levels of Cu(II) in their cerebrospinal fluid, and αS have been shown to have regulatory effect on calcium ions *in-vivo*. Copper has been found to have a very high affinity to several sites on the αS monomer, and ave been shown to accelerate fibrillation drastically. [4], [5]

In this study, we used a microfluidic, free-flow electrophoresis setup that previously has proven effective in measuring the net charge of αS monomers [6], [7], [8]. We looked at Cu(II) and Ca(II) ion interaction with αS monomers in the pH range 5.5 to 7. We measured the diffusion constant, using microfluidic diffusional sizing, and the electrophoretic mobility, using electrophoresis, of αS monomers labeled with Alexa488 in the context of the different ions and buffers, as well as a control experiment with unlabeled αS monomers using UV microscopy.

Table I: Overview of Samples

Name	pH	I	Divalent Cation
7	7.03	5 mM	
6.5	6.59	5 mM	
6	5.99	5 mM	
5.5	5.46	5 mM	
Ca7	7.03	5.3 mM	0.1 mM $CaCl_2$
Ca6.5	6.59	5.3 mM	0.1 mM $CaCl_2$
Ca6	5.99	5.3 mM	0.1 mM $CaCl_2$
Ca5.5	5.46	5.3 mM	0.1 mM $CaCl_2$
Cu7	7.03	5.3 mM	0.1 mM $CuCl_2$
Cu6.5	6.59	5.3 mM	0.1 mM $CuCl_2$
Cu6	5.99	5.3 mM	0.1 mM $CuCl_2$
Cu5.5	5.46	5.3 mM	0.1 mM $CuCl_2$

II. Materials & Methods

Sample Preparation

For the experiments, 12 different buffers were prepared. Each buffer contained 5 mM MES and 0.01% v/v tween20. The pH was adjusted with 1 M NaOH, and the ionic strength (I) was adjusted with NaCl. The sample contents and properties are shown in Table I.

Protein Preparation

αS was buffer exchanged from PBS to $NaHCO_3$ on amicon spin filter (3 kDa MW cutoff) to NaHC03 (pH 8.3). 5 molar equivalents of Alexa Fluor 488 NHS ester for N terminal amine labelling was added and solution was incubated over night at 4°C. αS solution was purified using size exclusion chromatogrphy on a Superdex 75 increase column. The label frequency was approximately 0.5 Alexa488 per αS.

Labelled and unlabelled αS was buffer exchanged to pure H_2O through 6 iterations of centrifuging in filter tube (21,000 rfc, 10 min, 3 kDa cutoff, 6°C), to a final buffer dilution of 1:5000. αS was shock-frozen and kept at -80°C for storage and thawed for use. The samples were never subject to more than four iterations of thawing and shock freezing.

Device Manufacturing

PDMS and cross-linker were mixed 10:1 and carbon black was added to the PDMS mixture. The PDMS mixture was centrifuged (40 min, 5000 rpm), added to masters and vacuumed for 3-10 hours. Masters were then baked (60-90 min, 65°C) and devices were cut out, punched, and cleaned in isopropanol using ultrasonic waves (12 min). Microscopy glass slides were cleaned by rubbing them with ethanol wipes and washed in isopropanol. Devices and glass slides were blow-dried. The glass slide and device surfaces were then activated using an

oxygen plasma oven (40% power, 30 s) (Deiner Electronics) and then bounded to each other. Finally, devices were post-baked (10-20 min, 65°C).

Diffusion Sizing

D6.0 device masters (designed by Herling [9]) were manufactured with SU3025 according to protocol with 60 s exposure to UV lamp. Devices were manufactured according to the protocol in *Device Manufacturing*, with 90 min of baking.

Before performing measurements, devices were incubated with buffer for at least 30 min.

Diffusion sizing measurements were performed with 4 μM αS, labelled with Alexa488, using a fluorescence microscope. For each measurement, three images were taken with 0.1 s - 1 s exposure time, and for each buffer, two measurements were performed using different flow rates were used (100 μl/h, and 200 μl/h). At least 3 minutes passed between inserting the sample into the device, and at least 6 minutes passed between switching flow rates. When changing buffer in a device, 80 μl buffer was flushed through to rinse the channels.

UV Diffusion Sizing

Devices were manufactured according to the protocol in *Device Manufacturing*, with 90 min of baking, but using quartz slides instead of glass slides.

Unlabeled αS monomers were concentrated from 300 μM to 1.2 mM through three iterations of centrifuging in a filter tube (13,000 rfc, 10 min, 3 kDa cutoff, 6°C). Samples were then diluted in the correct buffer to a monomer concentration of 450 μM.

UV sizing measurements were performed with 450 μM αS, in the same way as for the labelled measurements, but using flow rates of 150 μl/h and 250 μl/h. An exposure time of 10 s was required to yield any reasonable signal.

Sizing measurements were also performed using D6.0 devices on quartz with 450 μM labelled αS.

Labelled αS monomers were concentrated from 100 μM to 543 μM through four iterations of centrifugation in a filter tube (13,000 rfc, 10 min, 3 kDa cutoff, 20°C). Samples were then diluted in the correct buffer to a monomer concentration of 450μM.

Measurements were then performed identically to the previous diffusion sizing measurements using 50 ms exposure and flow rates of 100 μl/h and 200 μl/h.

Electrophoresis

E11.05 and E22.2 device masters were manufactured with SU3025 according to protocol, with 25 s exposure to UV. Devices were manufactured according to the protocol in *Device Manufacturing*, with 60 min of baking. Device electrodes (indium-arsenic alloy) were then inserted into the devices by heating the devices on a heated table (95°C), and wires were soled to the devices. All devices were tested by measuring the resistivity through the electrodes before use.

When performing microfluidic electrophoresis using solid electrodes, the device cell constant and the buffer conductivity need to be measured. To do so, the impedance over the device was measured for varying frequencies of AC (10 Hz-100 kHz, 10 mV) using a lock-in amplifier. This procedure will hereafter be referred to as the "impedance measurement". By performing the impedance measurement with a conductivity standard (500 μS), the device cell constant is calculated. By performing the impedance measurement on a buffer using a device with a known cell constant, the conductivity of the buffer is computed. The impedance measurement was performed on all devices and all buffers before the main electrophoresis experiments. When changing between the conductivity standard and buffer, the device was flushed with 100 μl/h water.

Electrophoresis measurements were performed with 5 μM αS, labelled with Alexa488, using a light microscope. The measurements were automated to perform three repeats of taking three images for each of 11 different voltages applied over the device channel, resulting in 99 images. The flow rate was 500 μl/h. When changing buffer in a device, 80 μl buffer was flushed through the device.

Analysis

All diffusion sizing images were analysed with the Diffusion Sizing script by Quentin Peter, and all electrophoresis images were analysed with the electrophoresis script by Therese Herling. Images were enhanced by smoothing and reducing background, before being sliced so that one-dimensional dispersions could be extracted. Mathematical functions describing the dispersion were then fitted against the one-dimensional slices (Figure 1a).

III. Results & Discussion

Diffusion Sizing

To determine the net charge of αS from the electrophoresis experiments, we first needed to measure the diffusion constant of αS in the different buffers. Figure 1 shows measured sizes for αS in each different buffer. As can be seen in Figure 2, the signal to noise ratio of the microscopy images was excellent, and the estimated standard deviation of the fitted size was around 2-5%. The absolute error between measurements with different flow rates was less than 7%, and between different devices, the standard deviation was less than 10%. The error bars in Figure 1 indicate the standard deviation of the measurements with the described errors propagated.

The measured radius of αS in buffer 7 compares well with previous measurements, which vary in the range 30 Å - 34 Å [10], [11]. Interestingly, Figure 1 indicate that the size of αS monomers increases with pH. At pH 6, there also seems to be a statistically significant difference in size between all three samples (No cations, Ca^{2+}, Cu^{2+}). These results were consistent between two repeats of the same experiments, performed on separate days, on different batches of αS, and different microscopes.

The size difference is significantly larger than previous reports of pH dependence, which measured a 2 Å difference between αS in pH 2.2 and 7.4 [11].

It was also noted that the fluorescence intensity drastically changed when Cu^{2+} was added. The exposure time used on samples with Cu^{2+} was therefore 2-3 times longer than on other samples. This is likely fluorescence quenching due to the αS-Cu^{2+} interaction. The lower intensity could also be explained by αS aggregation to fibrils, but we would then expect the calculated diffusion constant to be significantly larger.

A. UV Diffusion Sizing

As a way of measuring any potential effect that Alexa488 labelling might have on αS size in the different buffers, I performed a control experiment with unlabeled monomers using a UV microscope. As the inherent fluorescence of αS monomers is very poor, 450 μM αS was required in the measurement. Figure 3 shows an image from measurement on αS in buffer 6.5. Even with 10 s exposure time, the signal is poor (Figure 4a).

The standard error on the UV size measurements were large, but still consistently >5 Å smaller than the measured size for labeled αS at low concentrations (4 μM). The size of αS have previously been reported to be dependent on protein concentration (+1 Å per 100 μM in the range 100 μM - 300 μM, for unlabeled αS [10]). Therefore, a second control measurement with equally high concentration (450 μM) of Alexa488-labeled αS was performed. The comparison between the measured sizes from the UV measurements and the bright-field measurements can be seen in Figure 4. 450μM labelled monomers are consistently more than 5 Å larger than the unlabeled monomer at the same concentration. This could indicate that the Alexa488 label affect the shape of αS. Indeed, the hydrodynamic radius of Alexa488 is 5 Å. However, the difference could be a result of poor signal in the measurement. The hypothesis that the size difference is caused by poor signal is supported by the previous reports that 240 μM unlabeled αS has the hydrodynamic radius 30 Å $\pm$ 2 Å [10], which is 10 Å larger than what was obtained for the unlabeled monomers but in line with the results obtained from the labeled measurement.

Electrophoresis

Initially, buffer conductance was measured. The conductance is shown in Table II. One would expect the conductance of buffer Ca7 (366 μS) to be identical to the conductance of buffer Cu7 (460 μS). As no control experiments were performed, we will assume that there was some error when measuring the conductance of Ca7 and therefore use the value of 460 μS for Ca7 as well.

Table II: Measured Conductance of Three Buffers

Buffer	Conductance /μS
7	439
Cu7	460
Ca7	366

The cell constants for three devices was computed. Only two of these were actually used for measurements. Measured cell constants and which device was used for what can be seen in Table III.

Table III: Overview of Devices

Device	Cell Constant /cm^{-1}	Measurements on Buffer
E11.05	83.3	7, Cu7 & Ca7
E22.2 (1)	52.6	Ca7
E22.2 (2)	32.0	None

There are no results from measurements on device E22.2(2) as there was air in the channel. The errors from fitting the cell constants were 5%, but the issues when performing the measurement, such as air in the channel, are significantly greater although they can not be accurately quantified. One could argue that the cell constant of the E22.2 devices should be closer to 40 cm^{-1} as the channel in E22.2 is half of that in E11.05.

Sample images from the measurements on αS in buffer 7 can be seen in Figure 5. Most measurements were performed on the E11.05 device, but one was performed on an E22.2 device. Electrophoresis measurements were, due to lack of time, never repeated. Figure 6 shows the average particle deflection for αS in buffer 7, Ca7, and Cu7. No deflection was detected in Cu7. Using the measured deflection, cell constant, buffer conductivity, and diffusion coefficient, the electrophoretic mobility, and the net charge of the αS monomers are derived from:

$$\mu_e = \frac{v_e}{E}$$

$$n|e| = 6\pi R_H \eta \mu_e$$

where μ_e is the electrophoretic mobility, n is the net charge (in elemental charges, $|e|$), v_e is the measured electrophoretic velocity, E is the applied electric field strength, R_H is the hydrodynamic radius (measured in the diffusion sizing experiments, and η is the water viscosity.

Table IV shows the final computed net charges for all measurements. In order to calculate the true absolute charge of αS monomers, one would have to subtract the absolute charge of the label (-2 per Alexa488 at pH 7). The difference between the measurements with buffer Ca7 on the two different designs could be explained by poor measurements of the cell constants or air in the electrophoresis device. The measured value for αS in buffer 7 compares well with previous measurements on the same setup and measurements on different setups [6], [10]. For example, Wolff *et. al.* measured the net charge of Alexa488 labeled αS monomers at pH 7.4 to approximately -9 [6].

Due to time constraints, electrophoresis was only performed for αS in buffer 7, Ca7, and Cu7.

Table IV: Computed Electrophoretic Mobility and Net Charge

Measurement	μ_e /(μm/s)(V/cm)$^{-1}$	n /$\|e\|$
7	-2.33	-8.7
Cu7	-0.067	-0.2
Ca7	-2.79	-9.8
Ca7 (E22.2)	-1.55	-5.5

There is no apparent difference between the charge of αS in buffer 7 or Ca7. There is however, a significant difference between the computed charge of in buffer 7 and Cu7. The difference indicates that several copper ions are binding to the monomer at pH 7. One could speculate that this interaction partly explains the increased aggregation rate that is observed for αS in copper solutions. Binding of copper to αS could also explain the observed increased levels of copper that is observed *in-vivo* in PD patients.

IV. Conclusion

The goal of this project was to probe for, and characterise, interactions between αS monomers and divalent cations by measuring the net charge for αS monomers at different pH. Although few electrophoresis measurements were performed, some interesting findings can be noted.

- There is interaction between Cu(II) ions and αS monomers. Mainly, a significant number of experimental issues was noted during the project in various shapes and forms when Cu(II) ions were added to the monomers. Most convincing is the computed final charge on the αS monomers in buffer Cu7. Except for these observations, however, the interaction cannot be accurately described or quantified based on the limited studies of this project. Several of the issues could probably be explained by a accelerated fibrillation process, which has already been observed several times [5].
- No significant interaction between calcium ions and αS monomers could be detected in the experiments.
- αS monomer size seems to be pH dependent. It would be interesting to see if the charge also follows this dependency.
- There is a significant difference between UV measurements on unlabeled αS monomers and labelled αS monomers in buffer 7 at the concentration 450 μM. This could be because:
  - αS monomers do not yield significant signal in the UV microscope to enable accurate measurements.
  - There is an actual difference in size between labelled and unlabeled monomers at this concentration.

Suggestions for future follow-up experiments from the four findings include electrophoresis measurements for the remaining buffers, aggregation kinetics measurements for αS in buffer Cu5.5-7, NMR measurements to confirm the detected pH dependence and UV-microscopy measurements on labelled αS monomers. Repeats of the experiments performed would also be useful.

Acknowledgment

I am increadibly greateful for this oppurtunity given to me by Tuomas JP Knowles. Everyone working in the Centre for Protein Misfolding Diseases have been increadibly helpful and understanding when I have encountered problems. I am especially grateful for the introduction and instructions that I recieved upon arrival by Matthias Schneider, who also helped me with protein labeling and adviced me on experiment design.

References

[1] M. Bisaglia and L. Bubacco, "Copper ions and parkinson's disease: Why is homeostasis so relevant?" *Biomolecules*, vol. 10, no. 2, p. 195, Jan. 2020. [Online]. Available: https://doi.org/10.3390/biom10020195

[2] P. Faller, C. Hureau, and G. L. Penna, "Metal ions and intrinsically disordered proteins and peptides: From cu/zn amyloid- to general principles," *Accounts of Chemical Research*, vol. 47, pp. 2252–2259, 8 2014. [Online]. Available: https://pubs.acs.org/sharingguidelines

[3] E. Deas, N. Cremades, P. R. Angelova, M. H. Ludtmann, Z. Yao, S. Chen, M. H. Horrocks, B. Banushi, D. Little, M. J. Devine, P. Gissen, D. Klenerman, C. M. Dobson, N. W. Wood, S. Gandhi, and A. Y. Abramov, "Alpha-synuclein oligomers interact with metal ions to induce oxidative stress and neuronal death in parkinson's disease," *Antioxidants and Redox Signaling*, vol. 24, pp. 376–391, 3 2016. [Online]. Available: /pmc/articles/PMC4999647//pmc/articles/PMC4999647/?report=abstracthttps://www.ncbi.nlm.nih.gov/pmc/articles/PMC4999647/

[4] R. Moons, A. Konijnenberg, C. Mensch, R. V. Elzen, C. Johannessen, S. Maudsley, A.-M. Lambeir, and F. Sobott, "Metal ions shape -synuclein," *Scientific Reports*, vol. 10, no. 1, Oct. 2020. [Online]. Available: https://doi.org/10.1038/s41598-020-73207-9

[5] N. Bisi, L. Feni, K. Peqini, H. Pérez-Peña, S. Ongeri, S. Pieraccini, and S. Pellegrino, "-synuclein: An all-inclusive trip around its structure, influencing factors and applied techniques," *Frontiers in Chemistry*, vol. 9, p. 457, 2021. [Online]. Available: https://www.frontiersin.org/article/10.3389/fchem.2021.666585

[6] M. Wolff, J. J. Mittag, T. W. Herling, E. D. Genst, C. M. Dobson, T. P. Knowles, D. Braun, and A. K. Buell, "Quantitative thermophoretic study of disease-related protein aggregates," *Scientific Reports*, vol. 6, 3 2016.

[7] T. W. Herling, P. Arosio, T. Müller, S. Linse, and T. P. Knowles, "A microfluidic platform for quantitative measurements of effective protein charges and single ion binding in solution," *Physical Chemistry Chemical Physics*, vol. 17, pp. 12 161–12 167, 5 2015. [Online]. Available: www.rsc.org/pccp

[8] T. W. Herling, T. Müller, L. Rajah, J. N. Skepper, M. Vendruscolo, and T. P. J. Knowles, "Cite as," *Appl. Phys. Lett*, vol. 102, p. 184102, 2013. [Online]. Available: https://doi.org/10.1063/1.4803917

[9] Y. Zhang, T. W. Herling, S. Kreida, Q. A. Peter, T. Kartanas, S. Törnroth-Horsefield, S. Linse, and T. P. Knowles, "A microfluidic strategy for the detection of membrane protein interactions," *Lab on a Chip*, vol. 20, pp. 3230–3238, 9 2020. [Online]. Available: https://pubs.rsc.org/en/content/articlehtml/2020/lc/d0lc00205dhttps://pubs.rsc.org/en/content/articlelanding/2020/lc/d0lc00205d

[10] V. Ramanujam, T. R. Alderson, I. Pritišanac, J. Ying, and A. Bax, "Protein structural changes characterized by high-pressure, pulsed field gradient diffusion nmr spectroscopy," *Journal of Magnetic Resonance*, vol. 312, p. 106701, 3 2020.

[11] K. P. Wu, D. S. Weinstock, C. Narayanan, R. M. Levy, and J. Baum, "Structural reorganization of -synuclein at low ph observed by nmr and remd simulations," *Journal of Molecular Biology*, vol. 391, pp. 784–796, 8 2009.

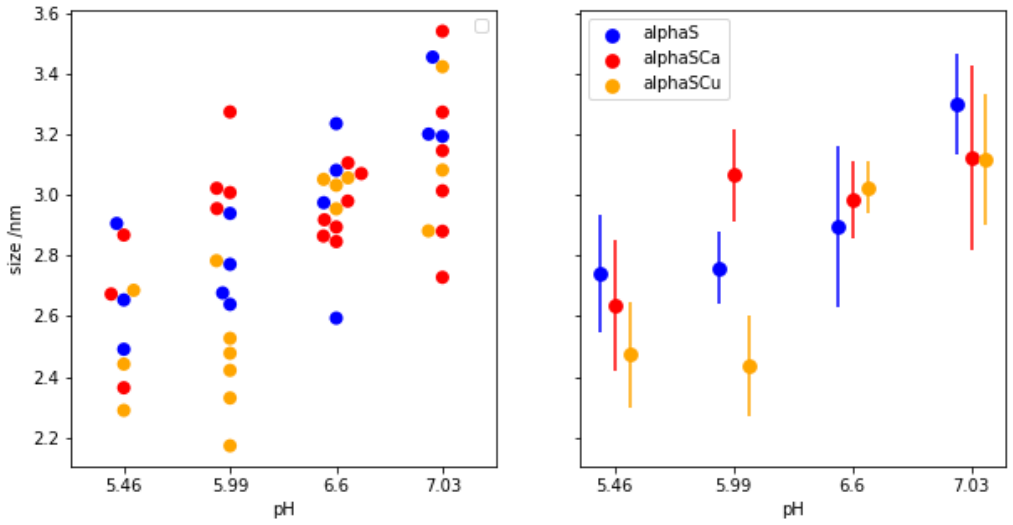

Figure 1: Hydrodynamic radius of αS at four different pH values. For each measurement on a unique device, averaged over different flow rates (**left**), and averaged across all devices and flow rates with propagated errors from fitting algorithms (**right**). **Blue**: 4 μM αS in buffer 7. **Red**: 4 μM αS in buffer Ca7. **Orange**: 4 μM αS in buffer Cu7.

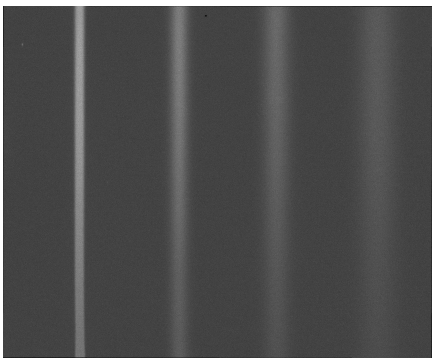

(a) Enhanced Microscopy Image

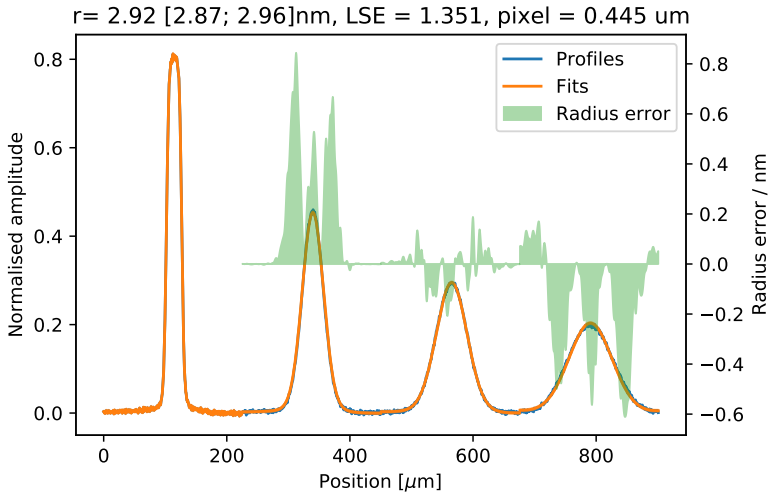

(b) Fitted Diffusion Data

Figure 2: Enhanced microscopy image (**left**), and extracted and fitted diffusion curves (**right**), from one measurement of 4 μM αS in buffer Ca7.

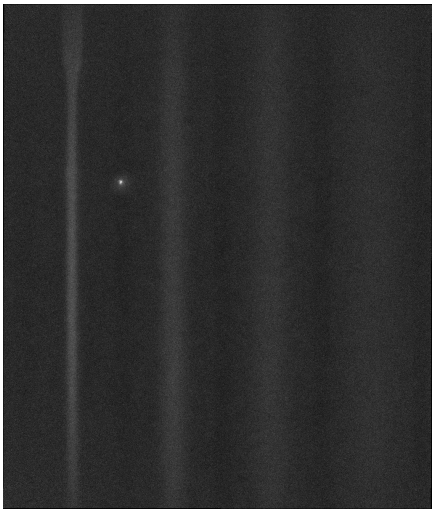

(a) Enhanced UV Microscopy Image

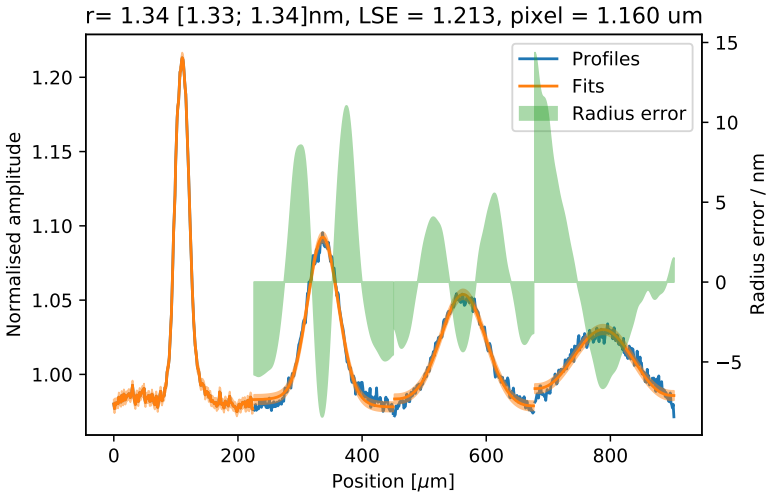

(b) Fitted UV Diffusion Data

Figure 3: Enhanced microscopy image (**left**), and extracted and fitted diffusion curves (**right**), from one UV measurement of 450 μM αS in buffer 6.5.

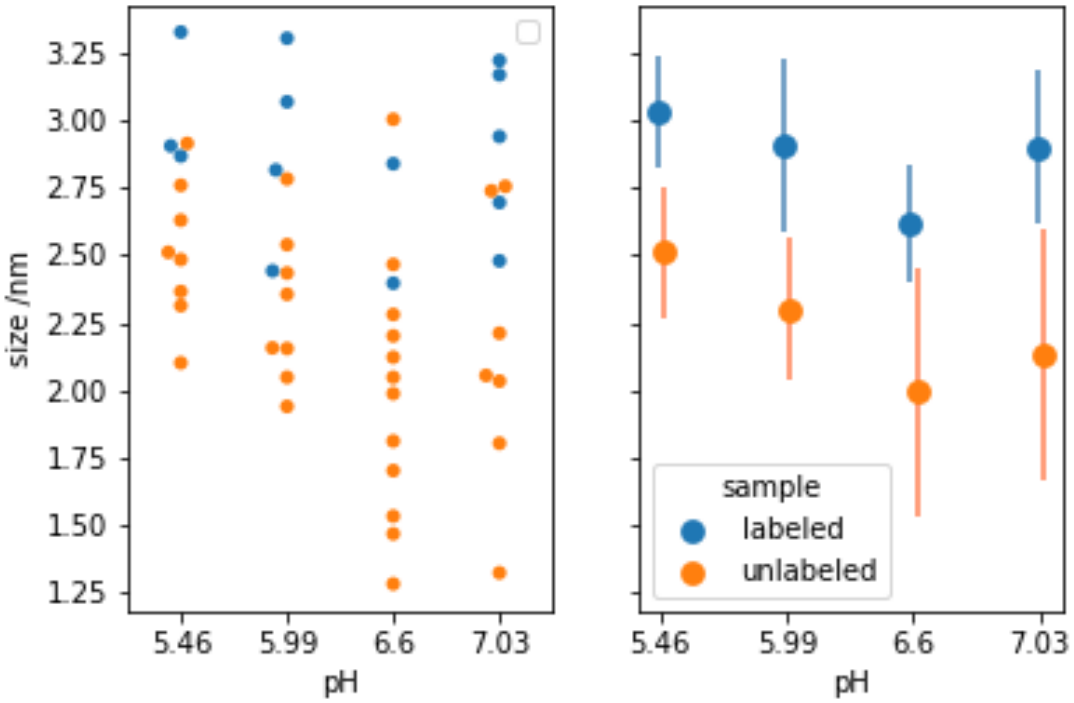

Figure 4: Hydrodynamic radius for 450 μM labeled (**Blue**), and unlabeled (**orange**) αS monomers at four different pH. **Left**: Each measurement on a unique device, averaged over different flow rates. **Right**: Average size across all devices and flow rates with propagated errors from fitting algorithms.

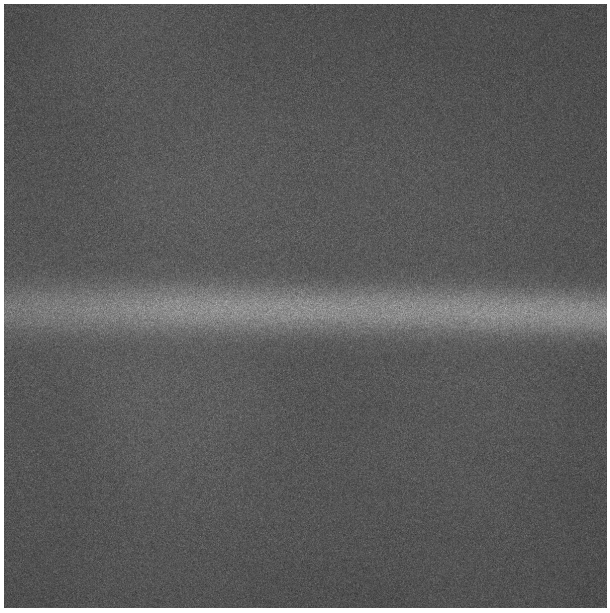

(a) Microscopy image with no voltage applied

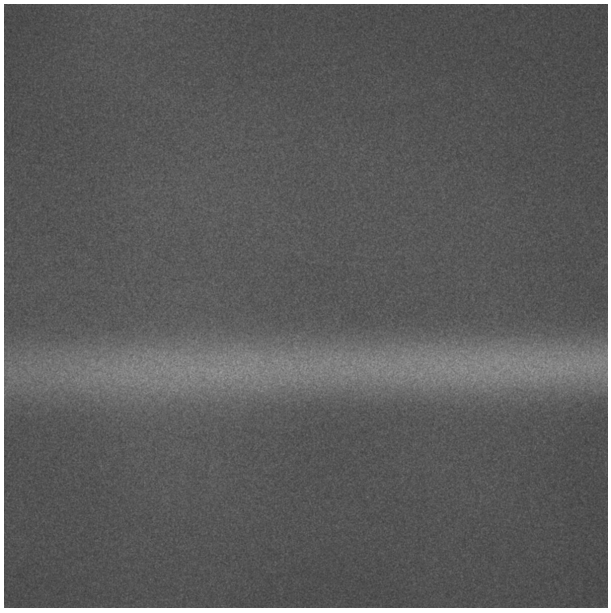

(b) Microscopy image with 5V applied

Figure 5: Enhanced microscopy image with no voltage applied over the channel (**left**), and with 5 V applied over the channel (**right**). The two microscopy images are taken in the exact same position.

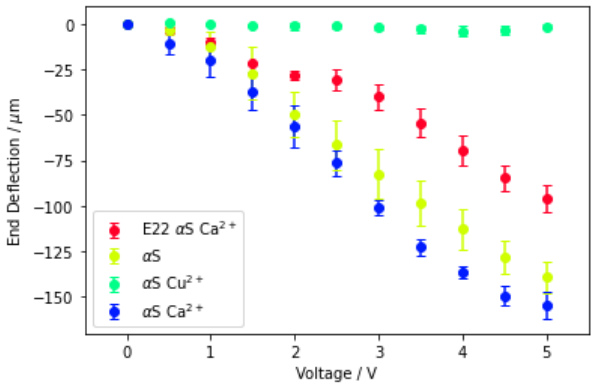

(a) Particle deflection against voltage

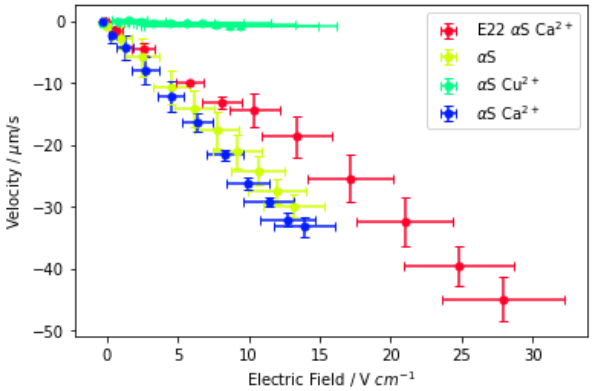

(b) Particle velocity against applied electric field strength

Figure 6: **Left**: Mean particle deflection against applied voltage. **Right**: Particle velocity against electric field strength. The velocity is computed from the deflection and device geometry, the electric field strength is computed from the applied voltage, the buffer conductance, the device cell constant and the device geometry. **Red**: αS in buffer Ca7, measured on device E22.2. **Yellow**: αS in buffer 7, measured on device E11.05. **Green**: αS in buffer Cu7, measured on device E11.05. **Blue**: αS in buffer Ca7, measured on device E11.05. Mean deflection was computed by extracting the maximum of the diffusion profile.